RESEARCH ON EXPERIMENTAL STUDY OF PRESSURE-INDUCED DAMAGE OF PULMONARY ARTERY FOR PULMONARY HYPERTENSION

By

Yuheng Wang

A THESIS

Submitted to
Michigan State University
in partial fulfillment of the requirements
for the degree of

Mechanical Engineering – Master of Science

ABSTRACT

RESEARCH ON EXPERIMENTAL STUDY OF PRESSURE-INDUCED DAMAGE OF PULMONARY ARTERY FOR PULMONARY HYPERTENSION

By

Yuheng Wang

Pulmonary hypertension (PH) is associated with elevated pulmonary arterial pressure. PH prognosis remains poor with 15% mortality rate within 1 year even with modern clinical managements. Previous clini cal studies proposed the wall shear stress (WSS) to be an important hemodynamic factor for affecting cell mechanotransduction and growth and remodeling in the disease progress. However, a typical range of WSS in vivo is at most 2.5 Pa and a doubt has been casted whether WSS alone can influence the disease progress. Furthermore, our current understanding of PH pathology has largely been obtained through small animals and there has been seldom reports of caliber enlargement in the PH animal models. Therefore, a large-animal experiment on pulmonary arteries (PAs) is needed for validating whether an increased pressure can induce an enlargement of pulmonary caliber. In this study, we use an inflation testing device to characterize the mechanical behavior, both nonlinear elastic behavior and irreversible damage of porcine arteries. The parameters of elastic behavior are estimated from the inflation test at a low-pressure range first and then are compared with those from a high-pressure range, which tests if those behavior are significantly different. At the end of mechanical tests, histological images are qualitatively examined for medial and adventitial layers. This study, therefore, sheds light on the relevance of pressure-induced damage mechanism in human PH

ACKNOWLEDGEMENTS

During my M.S. program, I met many people who helped and encouraged me. First, I would like to thank my primary advisor Dr. Sara Roccabianca who gives me a great opportunity to do the research in her group as master student. I am very grateful to her encouragement, inspiration and knowledge support through my entire master program. I would also like to thank my committee member Dr. Seungik Baek and Dr. Lik Chuan Lee for their constructive guidance and valuable feedback.

I also appreciate all the members from our research group Dr. Sheng Chen, Dr. Hamidreza Gharahi, Marissa Rae Grobbel, Mayank Sinha, Tyler Tuttle and Laura Alison Nye. They have contributed a lot to my research. As co-workers, they provided a lot of technic supports and suggestions while doing the experiment.

Finally, special thanks should belong to my lovely family and friends for their unconditional supports and encouragement

TABLE OF CONTENTS

LIST OF TABLES	v
LIST OF FIGURES	vi
CHAPTER 1: Introduction and literature review	1
1.1 Overview	1
1.2 Arterial mechanics and its role in the progression of cardiovascular pathology	2
1.3 Pulmonary artery microstructural organization in healthy and PH	6
1.4 Pulmonary artery constitutive model	10
1.5 Mechanical test of elastic vessels in vivo and in vitro	15
CHAPTER 2 : Mechanical characterization of damage behavior in the pulmonary artery	17
2.1 Introduction	
2.2 Methods	17
2.2.1 Specimen preparation	17
2.2.2 Mechanical testing	
2.2.3 Histological analysis	
2.2.4 Mechanical model	
2.3 Results	21
2.4 Discussion	27
2.5 Conclusion	
BIBLIOGRAPHY	32

LIST OF TABLES

Table 1. Best-fit material parameters for the 2-fiber family model and estimated axial stretch.. 27

LIST OF FIGURES

Figure 1. Schematic of the layered microstructure of the arterial wall. (G. A. Holzapfel, Gasser, & Ogden, 2000)
Figure 2. Contour plot of the convex potential (1) with material parameters a = 44.2 kPa and b = 16.7 (see (Delfino et al., 1997))
Figure 3 . Contour plots of the potential (3) with (a) material parametersc, $b_1,, b_7$ in (Chuong & Fung, 1983), and (b) a set of parameters chosen to illustrate non-convexity
Figure 4 . Inflation-extension testing device with specimen mounted in between
Figure 5 . Luminal pressure and outer diameter raw data for a representative sample, as collected throughout the mechanical test. Specifically, part 1 (dark gray line) describes the mechanical behavior of the PA before the damage, part 2 (light gray line) describes the response to overpressurization which generates damage within the wall, and part 3 (dark gray line) describes the mechanical behavior of the PA after damage. Also shown, the preconditioning protocol (dotted light gray line).
Figure 6 . Average pressure vs. normalized diameter curve for all specimens. D_B and D_A correspond to before and after damage diameters, respectively. The before damage behaviors have been collected during the first loading of part 1 of the test, while the after damage behavior have been collected during part 3 of the test. The asterisk indicates that the normalized diameters were significantly different, at $p < 0.05$, when comparing before and after damage behaviors 24
Figure 7 . Change in diameter during different loading curves. Black circles represent that diameter difference between the first and second loading curve of part 2 of the test, gray squares represent the difference in diameter between the second and third loading curve. The \ast indicates that the diameters were significantly different at p < 0:05
Figure 8 . Histology images of tissue samples from the PA. Top row: Picrosirius red under polarized light (collagen fibers in red, yellow and green); bottom row: VVG (elastin in black, nuclei in purple, and cytoplasm in pink). Left: before damage samples; right: after damage samples. Bar in each image represents 500 μm

CHAPTER 1: Introduction and literature review

1.1 Overview

Pulmonary hypertension (PH) is a type of high blood pressure that affects the right ventricle and the arteries in the lungs. PH can develop without a known cause (primary pulmonary hypertension) or as a result of other diseases (secondary pulmonary hypertension). Secondary pulmonary hypertension is often associated with collagen vascular disease, chronic thromboembolism, human immunodeficiency virus, and other diseases. Prognosis is severe in PH and when untreated it is a potentially fatal disease that rapidly leads to disability and premature mortality (Stepnowska, Lewicka, Dabrowska-Kugacka, Miękus, & Raczak, 2017). Since 1999, the number of deaths and hospitalizations as well as death rates and hospitalization rates for PH have increased. Despite improvements in the diagnosis and management of PH over the past 2 decades, with the introduction of targeted medical therapies leading to improved survival, the disease continues to have a poor long-term prognosis (Mehari, Valle, & Gillum, 2014). Further, the reversibility of PH is dependent on the relative contribution of vasoconstriction (reversible) and structural changes in the pulmonary vessels (mostly irreversible) (Rounds & Hill, 1984). Furthermore, when patients have symptoms or signs of PH, the disease is usually at an advanced stage, at which the pulmonary vasculature already shows remodeling in terms of the wall microstructure. Therefore, it is vital to determine the bio-chemo-mechanical processes involved with the initiation and progression of microstructural remodeling associated with PH, in order to prevent irreversible outcomes. Furthermore, a better understanding of the mechanisms that contributes to wall remodeling in PH could lead to innovative therapeutic targets.

1.2 Arterial mechanics and its role in the progression of cardiovascular pathology

Arteries have, primarily, a mechanical function, which is influenced heavily by the vessels' mechanical characteristics. Furthermore, it has been hypothesized that perturbations of the mechanical homeostatic state in arteries could be a driving force of disease progression. For example, data suggests that pressure-induced stress concentrations may play an important role in the formation and progression of atherosclerotic plaques (Thubrikar & Robicsek, 1995). In addition, it is widely accepted that arterial stiffening plays an important role in hypertension progression (Mitchell et al., 2010). A large longitudinal study recently established that arterial stiffening precedes an increase in systolic blood pressure, while initial blood pressure was not independently predictive of subsequent aortic stiffening (Kaess et al., 2012). These studies highlighted the importance of understanding the mechanisms underlying the initiation and progression of arterial stiffening in relation to hypertension, and of determining the temporal relationship between the development of arterial stiffness, high blood pressure, and cardiovascular disease (Weisbrod Robert M. et al., 2013). Finally, many researchers suggested that arterial wall mechanical dysfunction is one of the crucial mechanisms in the formation of abdominal aortic aneurysms (AAA). AAA are associated with atherosclerosis, aging, smoking, and hypertension, but the mechanism underlying the development of atherosclerotic aneurysms is not well understood (Hammond & Garfinkel, 1969). Previous studies observed that the formation of atherosclerotic aneurysm is associated with dramatic changes in the extracellular matrix composition and organization of the arterial wall. Collagen concentration has been found to be deficient (R. J. Rizzo et al., 1989), unchanged (Dubick, Hunter, Perez-Lizano, Mar, & Geokas, 1988), or increased (Menashi, Campa, Greenhalgh, & Powell, 1987) in atherosclerotic abdominal aortic aneurysms, whereas elastin concentration has been found to be consistently deficient in

aneurysms (Campa, Greenhalgh, & Powell, 1987; Dubick et al., 1988; Robert J Rizzo et al., 1989). From these studies it appears that an imbalance between synthesis and degradation of arterial connective tissue (collagen and elastin) may be responsible for the development of atherosclerotic aneurysms.

<u>Pulmonary hypertension: the biomechanical hypothesis.</u> Several hypotheses have been made to explain the mechanisms that lead to arterial mechanical dysfunction that aggravate, or possibly trigger, PH. These are complicated by the multifactorial nature of the disease, involving: (1) maladaptive pulmonary wall remodeling that leads to media hypertrophy, adventitial thickening and neointimal lesions (Botney, 1999); (2) degradation of molecular tissue components linked with age-related changes (Akhtar, Sherratt, Cruickshank, & Derby, 2011); and (3) mechanical damage mechanism triggered by abnormally large stresses exerted by hemodynamic forces (Zambrano et al., 2016, Humphrey & Tellides, 2018). Although the initiating mechanism of PH is still unclear, it is commonly accepted that hemodynamic conditions, especially wall shear stress (WSS), influence cardiovascular disease by affecting cell mechanotransduction and microstructural remodeling. There is increasing evidence, in the systemic vasculature, that low WSS is a promoter of increased wall stiffness and atherogenic vascular states, and could be an independent predictor of cardiovascular mortality (Cunningham & Gotlieb, 2005). Furthermore, recent studies proposed that WSS is the primary mechanical force affecting cell mechanotrasnduction in PH (Bürk et al., 2012), causing inflammatory response and change in cell expression from contractile to proliferative (Li, Scott, Shandas, Stenmark, & Tan, 2009; Li, Stenmark, Shandas, & Tan, 2009). Numerical studies suggested that a 30% increase in flow rate produces a 9% increase in arterial diameter (Valentín A, Cardamone L, Baek S, & Humphrey J.D, 2009), however, it has been showed experimentally that the increase in caliber of human pulmonary artery (PA) in PH patients

is significantly larger than that. Specifically, people affected by PH present more than 50% larger pulmonary artery's diameters when compared to healthy subjects in young patients (Truong et al., 2013), and 30 % in adults patients (Edwards, Bull, & Coulden, 1998). Clearly, diameter enlargement is one of the most prominent feature of PH and the distribution of WSS was found to have substantial influence on both the diameter and the shape of the vessels in the lungs (Vorp, Wang, Webster, & Federspiel, 1998), yet it seems improbable that low WSS alone could be responsible for the significant increase in arterial caliper in PH. Furthermore, previous studies also suggested that changes in the mechanical characteristics of the arterial wall could be involved in aggravating PH pathology. For example, Sanz and colleagues observed that, in exercise-induced PH, the pulmonary arteries' stiffness increase preceded the observation of an increase in both pressure and luminal diameter (Sanz et al., 2009). The Authors of that study suggested that an interplay between variations of wall stiffness, luminal diameter, and wall shear stress, as opposed to one isolated cause, could be at the root of PH progression. In this study, we hypothesize that a damage mechanism could also contribute to irreversible diameter enlargement in PH. To test this hypothesis, we combined in vitro experiments and theoretical modeling to investigate the role of damage in the mechanics of pulmonary artery.

<u>Damage mechanisms in elastic arteries.</u> Little is known about the response to damage of pulmonary arteries, however some studies focused on investigating damage mechanisms in other elastic arteries, both theoretically and experimentally. In 1987, one of the first attempts to model arterial wall damage at large strains was pursed by Simo (Simo, 1987). The author proposed a nonlinear viscoelastic constitutive model, capable of accommodating general anisotropic response and relaxation functions. This viscoelastic model successfully predicted the progressive loss of stiffness and increasing dissipation with increasing maximum amplitude of strain energy, which is

in agreement with the so-called Mullin's effect. Experimentally, Sommer and colleagues (Sommer, Regitnig, Költringer, & Holzapfel, 2009) performed quasi-static extension-inflation tests at human common carotid arteries to understand the mechanical behavior of a vessel subject to loads beyond the physiological domain. The results if this study showed that the burst pressure of ~60 kPa (~450 mmHg) may lead to damage or rupture of human carotid media-intima. A similar study, performed on human left anterior descending coronary arteries (Gerhard A. Holzapfel, Sommer, Gasser, & Regitnig, 2005), identified the "jacket like" behavior of the adventitial layer at higher pressure that prevent artery from overstretch and rupture. Finally, several previous experimental and numerical studies have demonstrated that central arteries could sustain blood pressure values > 200 mmHg, without sustaining damage (Ferrara & Pandolfi, 2008a; Martin, Sun, Pham, & Elefteriades, 2013), which is well over the physiologic range (Ferrara & Pandolfi, 2008b). While pulmonary arterial pressure is approximately one sixth that of the systemic pressure (Lammers et al., 2012), we do not know if the mechanical strength of the pulmonary arterial wall is comparable to other elastic arteries.

There are important aspects of the mechanics of pulmonary arteries, which could be contributing to PH initiation and progression, which have yet to be addressed. The goal of this dissertation is to investigate the irreversible mechanical damage that occurs in pulmonary arteries when subjected to supra-physiological loading conditions. We aim to achieve this goal by completing the following objectives

- To characterize experimentally the elastic and inelastic (irreversibly damaged) mechanical behavior of pulmonary arteries;
- 2) To identify changes in the arterial wall microstructure associated with damage, using modeling and histological analysis.

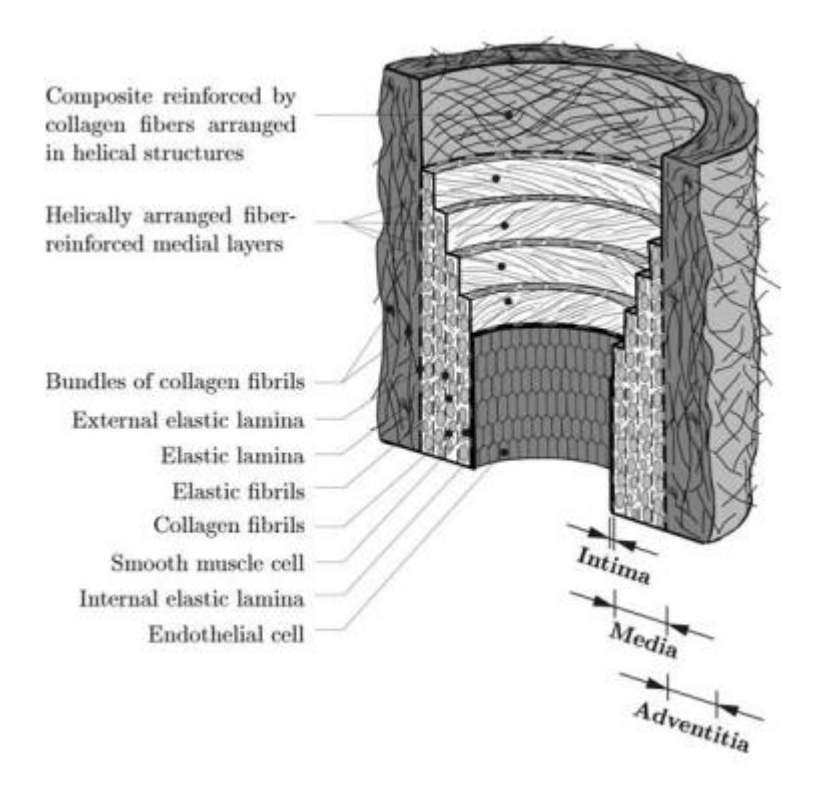


Figure 1. Schematic of the layered microstructure of the arterial wall. (G. A. Holzapfel, Gasser, & Ogden, 2000).

1.3 Pulmonary artery microstructural organization in healthy and PH

Arterial wall microstructure. The wall of elastic arteries, including the pulmonary artery, is made of three layers. The layers are identified as intima, media and adventitia, form the innermost (luminal) to the outermost, see **Figure 1**. The intimal layer, or tunica intima, consists of a thin layer of endothelial cells that are in direct contact with the blood flow. The medial layer, or tunica media, is composed of a series of concentric layers of elastic lamina alternated with layers of vascular smooth muscle cells (i.e., cells that have the ability of synthetizing proteins and of generating force by contracting). The elastic laminae are made of tightly packed elastin fibers and microfiblis. The smooth muscle cells and the elastin lamina are connected by radially oriented

fibers that allow the cells to sense their mechanical environment. The adventitial layer, or *tunica adventitia*, is composed of a three-dimensional network of connective tissue, mostly collagen type I and III, and fibroblasts (i.e., cells that have the ability of synthetizing structural proteins such us collagen fibers). The collagen fibers in the adventitia are somewhat organized along two preferential directions, which are at an angle (~ 45°) with respect to the vertical axis. This results in a three-dimensional spiral-shaped organization of bundles fibers, which can be referred to as "fiber families". The collagen bundle has a coiled structure that will increasingly straighten with increased loading.

<u>Structural function of the wall layers</u>. The intimal layer is thought to not have a considerable contribution to the mechanical behavior of elastic arteries. The medial layer gives the artery its strength and its elastic behavior, it is significantly engaged in the homeostatic range of loading, and it offers resistance to both longitudinal and circumferential loads. These behaviors are due to the presence of elastin fibers within the media. The adventitia is mostly engaged at higher values of stresses, it is thought to act as a protective sheath against over- pressurization (Bellini, Ferruzzi, Roccabianca, Di Martino, & Humphrey, 2014). This behavior is mostly associated with the structural recruitment of the embedded wavy collagen bundles, and it is generally though to lead to the characteristic anisotropic mechanical behavior of arteries (G. A. Holzapfel et al., 2000). Because of this microstructural organization, healthy elastic arteries behave as deformable composite structures, showing a highly nonlinear response and a stiffening effect at higher pressures. Furthermore, not just the organization of each constituent separately, but the balance of different constituents within the wall, has been thought to contribute significantly to the mechanical behaviors of healthy arteries (Armentano et al., 1991). However, in diseased arteries, this microstructure could be disrupted, leading to the inability of arteries to efficiently perform

their mechanical function. Therefore, to understand arterial dysfunction, due to long term remodeling of the wall or due to damage mechanisms, it is crucial to investigate and quantify changes in the microstructure of each constituent.

<u>Structural function of extracellular matrix fibers.</u> Collagen and elastin are the major load bearing constituents of the arterial wall. Specifically, the collagen fibers network has a stiff non-linear behavior, and the elastin fiber network shows a more compliant linear elastic behavior (Roach & Burton, 1957). In their seminal paper, Roach and Burton employed constituents' selective digestion to understand the role played by the collagen and elastin fiber network in defining the overall arterial behavior by isolating their contribution. Specifically, employing chemical degradation of collagen fibers and elastin fibers in iliac arteries followed by mechanical testing, they concluded that most of the mechanical behavior of arteries at lower values of pressure is ascribed to elastin, while most of the mechanical behavior at high values of pressure is influenced by collagen fiber network. Another study by Wagenseil and colleagues (Wagenseil & Mecham, 2012) reviewed the mechanical properties and contribution of elastic fibers to arterial stiffness, using genetically modified mice. First, they recognized that elastin fibers played a crucial role in influencing not just the mechanics of the wall but also cell behavior. They observed that elastin knockout (Eln-/-) mice die within a few days after birth because of the remarkably increase of cell number within the arterial wall, which obstructed the arteries. They also observed significant differences in incremental arterial stiffness between elastin knockout and wild type animals, despite the differences of aortic diameter at systole are minor in all genotypes, but the change in diameter between systole and diastole is approximately three times less in elastin knockout mice. Then, mice have been generated that express human elastin in a bacterial artificial chromosome (BAC-ELN). These animals are characterized by an increase in elastin amount from 30% to 120%

of normal levels. The results of this study suggested that elastin density is inversely proportional to arterial stiffness and blood pressure. All these studies taken together explained the mechanical role of the most relevant extracellular matrix components in the arterial wall, collagen and elastin. Damage modeling in soft tissues typically tends to be phenomenological, which requires the related parameters to be adjusted to specific experiments. Here, we propose to employ a micromechanically motivated approach to describe vessels before and after damage, to provide some physical interpretability of damage mechanism (Schriefl, Schmidt, Balzani, Sommer, & Holzapfel, 2015).

Changes of microstructural organization in PH. Previous pathological studies mainly established the relationship between hemodynamic factors and the change in the mechanical properties of tissues (Humphrey, Baek, & Niklason, 2007; Sheidaei, Hunley, Raguin, & Baek, 2009; Sho et al., 2004; Zambrano et al., 2016). Only few studies that relate pressure-induced microstructural change to the changes in the mechanics of the arterial wall. Until recent years, Bloksgaard claimed the first study that quantitatively relate pressure-induced microstructural changes in resistance arteries to the mechanics of their wall. Both modeling and imaging data suggested that the acute pressure-induced structural changes of human pericardial resistance arteries (hPRA) are small (Bloksgaard et al., 2017). In addition, Sanz et al. (Sanz et al., 2009) found that in exercise-induced PH patients, the pulmonary artery stiffness increased without significant change of luminal diameter. An accurate representation of the effect of damage on each PA's wall microstructural components is important to investigate PH, for the following reasons:

(1) *Different mechanical functions of artery*. Arteries is a multi-layered material consists of numbers of different constituents. Especially collagen fibers in artery, which is predominantly present in the adventitia as a dense network and is believed to have a load-bearing function.

The collagen configuration evolves continuously until rupture occurs (Schrauwen et al., 2012). Hence the pressure induced change of collagen network maybe monitored in over pressurizing procedure;

(2) Different mechanical response of subject. Current understanding of PH pathology has largely been obtained through small animal models in which there has been seldom reports of caliber enlargement (Nickel et al., 2015). Furthermore, permanent damage in healthy subject is not very common, the vessel wall damage has been reported in *in vitro* test (Wulandana & Robertson, 2005) and pathological conditions. Thus, experiments on pulmonary arteries in large animals are need for validation whether pressure alone can induce an enlargement caliber.

1.4 Pulmonary artery constitutive model

Constitutive models describing the mechanical properties of elastic arteries have been used to predict or investigate changes associated with disease initiation of progression. For example, models can predict blood flow and pressure, wall distension, normal and shear stresses, and energy requirements in elastic arteries, including the pulmonary vasculature. The choice of an appropriate constitutive model, however, is complicated by the complex wall structure of elastic arteries, that dictates passive mechanical behaviors of these vessels (Hunter, Lammers, & Shandas, 2011). The constitutive models can be categorized into two types: phenomenological and structural models. Phenomenological models are mathematical expressions that describe the behavior of vessels independently of any particular anatomical or physiological parameters. Delfino et al. (Delfino, Stergiopulos, Moore, & Meister, 1997) proposed an isotropic rubber-like strain energy potential to describe carotid arteries. This strain energy function Ψ, which is able to model the typical stiffening at high pressures, has the form

$$\Psi = \frac{a}{b} \{ \exp\left[\frac{b}{2} \left(\overline{I_1} - 3\right)\right] \},\tag{1}$$

where a>0 is a stress-like material parameter, b>0 is a non-dimensional parameter, and the first invariant of the modified Cauchy-Green deformation tensor $\overline{\textbf{\textit{C}}}$ is defined as $\overline{I}_1=tr(\overline{\textbf{\textit{C}}})$.

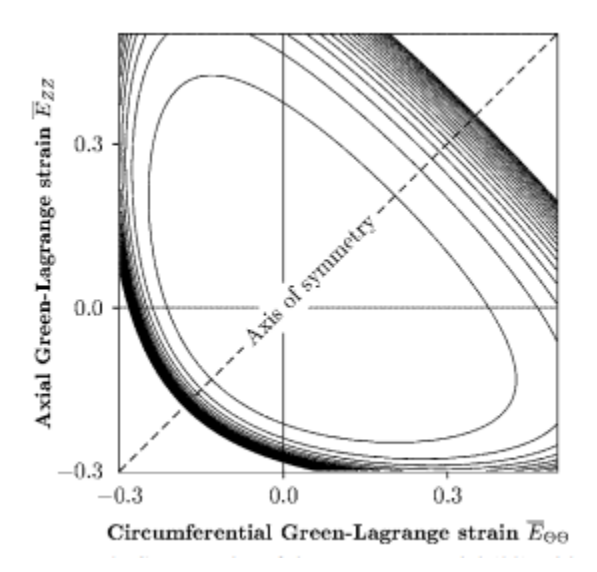


Figure 2. Contour plot of the convex potential (1) with material parameters a = 44.2 kPa and b = 16.7 (see (Delfino et al., 1997))

Another phenomenological strain energy function form have been introduced by Humphrey (Humphrey, 1995), and has the form

$$\bar{\psi} = \frac{1}{2}c \left[\exp(Q) - 1 \right], \tag{2}$$

where c is a material parameter (dimension of a stress) and Q is given by

$$Q = b_1 \bar{E}_{\Theta\Theta}^2 + b_2 \bar{E}_{ZZ}^2 + b_3 \bar{E}_{RR}^2 + 2b_4 \bar{E}_{\Theta\Theta} \bar{E}_{ZZ} + 2b_5 \bar{E}_{ZZ} \bar{E}_{RR}$$
$$+2b_6 \bar{E}_{RR} \bar{E}_{\Theta\Theta} + b_7 \bar{E}_{\ThetaZ}^2 + b_8 \bar{E}_{RZ}^2 + b_9 \bar{E}_{R\Theta}^2, \tag{3}$$

where b_i , i = 1, ..., 9 are non-dimensional material parameters, while \bar{E}_{IJ} , for $I, J = R, \Theta, Z$, are the components of the modified Green-Lagrange strain tensor referred to cylindrical polar coordinates (R, Θ, Z) . The modified Green-Lagrange strain tensor $\bar{\mathbf{E}}$ can be written as

$$\bar{\mathbf{E}} = \frac{1}{2}(\bar{\mathbf{C}} - \mathbf{I}),\tag{4}$$

where I denotes the second-order identity tensor, and $\bar{\textbf{C}}$ denotes the right Cauchy-Green tensor, defined as

$$\bar{\mathbf{C}} = \bar{\mathbf{F}}^{\mathrm{T}}\bar{\mathbf{F}}, \tag{5}$$

where $\bar{\mathbf{F}}$ represents the modified deformation gradient, defined to satisfy the relation $\mathbf{F} = (J^{1/3})\bar{\mathbf{F}}$ (\mathbf{F} represent the deformation gradient in large deformation). Compared to the work of Delfino, this strain energy function has no a priori restriction on the material parameters presented by assuming the artery is homogenous and incompressible.

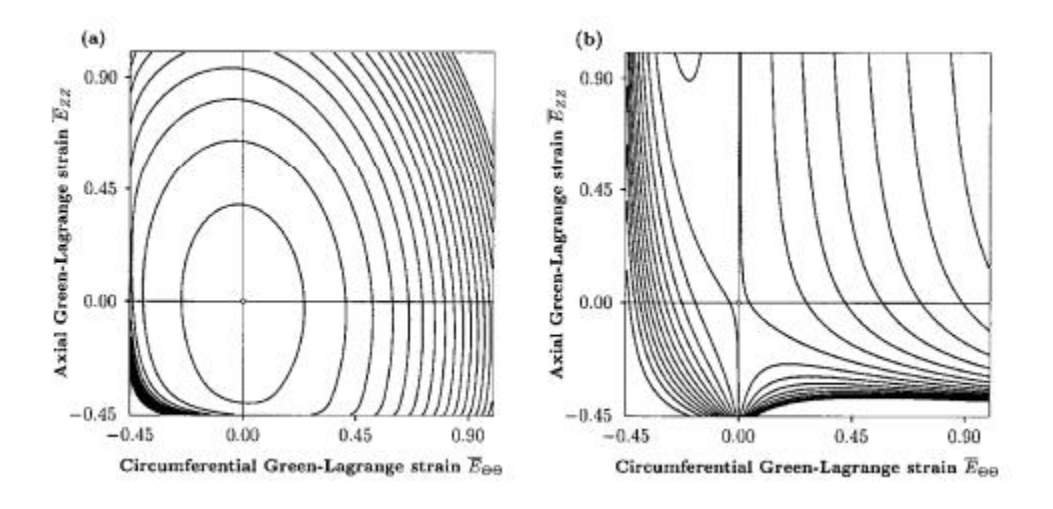


Figure 3. Contour plots of the potential (3) with (a) material parameters c, b_1 , ..., b_7 in (Chuong & Fung, 1983), and (b) a set of parameters chosen to illustrate non-convexity.

Finally, another well-known form of strain energy function for arteries is the one proposed by Takamizawa and Hayashi (Takamizawa & Hayashi, 1987) it has the logarithmic form

$$\hat{\bar{\psi}} = -c \ln(1 - \psi) , \qquad (6)$$

where c is a stress-like material parameter and the function ψ is given in the form

$$\psi = \frac{1}{2}b_1\bar{E}_{\Theta\Theta}^2 + \frac{1}{2}b_2\bar{E}_{ZZ}^2 + b_4\bar{E}_{\Theta\Theta}\bar{E}_{ZZ},\tag{7}$$

where b_1, b_2 , b_4 are non-dimensional material parameters and $\bar{E}_{\theta\theta}$, \bar{E}_{ZZ} are the components of the modified Green-Lagrange tensor \bar{E} in the circumferential and axial directions, as defined in Eq. (4). Due to the logarithmic form, in the particular condition = 1, the value $\hat{\psi}$ is infinite. Additionally, $\psi > 1$ would lead to an undefined function of $\hat{\psi}$. Therefore, this type of strainenergy function is only applicable for a limited range of states of deformation. Due to the strong influence of residual stresses, if (4) is used within a (displacement-driven) finite element formulation, may lead to numerical difficulties (G. A. Holzapfel et al., 2000).

The strain energy functions discussed above have the benefit of describing accurately the mechanical behavior of arteries. Due to their phenomenological nature, however, these descriptions are lacking connection with anatomic and physiologic quantities, significantly reducing the opportunity for independent validation of parameters (Hunter et al., 2011). In the last 20 years, however, there has been an effort to incorporate microstructural information in the mechanical modeling of arteries. Holzapfel and Gasser first introduced these concepts, inspired by the mathematical methods used to describe fiber-reinforce and multi-laminated composites (G. A. Holzapfel et al., 2000; Hunter et al., 2011). Briefly, the basic idea is to include histological information within the constitutive model so that the material parameters could be connected with

microstructural components' density and organization. For the first time, the Authors introduced the idea of modeling the arterial wall as a bilayered structure, where each layer is made of fiber-reinforced elastic materials with different characteristics. For example, the medial layer, which is mostly comprised of elastin, is described by an isotropic material description, while the adventitial layer, which is mostly made of collagen fibers, is endowed anisotropic mechanical behaviors. Finally, the anisotropic and isotropic parts are summed together using the concepts of the traditional mixture theory,

$$\bar{\psi}_{Holz} = \bar{\psi}_{iso} + \bar{\psi}_{aniso}. \tag{8}$$

Specifically, in (G. A. Holzapfel et al., 2000; Hunter et al., 2011)the isotropic portion is described employing a neo-Hooken model

$$\bar{\psi}_{iso}(\bar{I}_1) = \frac{c}{2}(\bar{I}_1 - 3), \qquad (9)$$

where c > 0 is a stress-like material parameter. While the collagen fibers are described by an exponential strain energy function, to represent the stiffening behavior at higher pressure, as follows

$$\bar{\psi}_{iso}(\bar{I}_4, \bar{I}_6) = \frac{k_1}{2k_2} \sum_{i=4,6} \{ \exp[k_2(\bar{I}_i - 1)^2 - 1]$$
 (10)

where $k_1 > 0$ is a stress-like material parameter and $k_2 > 0$ is a dimensionless parameter. Note that $\overline{I_4}$ and $\overline{I_6}$ are the squares of the stretches in the direction of A_1 and A_2 , that characterize the direction of two (reference) fiber families. Therefore, the reduced from is given by

$$\bar{\psi}(\bar{\mathbf{C}}, \mathbf{A_1}, \mathbf{A_2}) = \bar{\psi}_{iso}(\bar{I}_i) + \bar{\psi}_{aniso}(\bar{I}_4, \bar{I}_6). \tag{11}$$

Based on the strain-energy function proposed by Holzapfel and Gasser (G. A. Holzapfel et al., 2000), this dissertation will focus on determine the constituent-wise indication of the damage

of the pulmonary arterial wall. Collagen fiber stiffness parameter and fiber direction will also be estimated from the experimental data and histological images.

1.5 Mechanical test of elastic vessels in vivo and in vitro

Cyclic inflation test has been employed in several previous studies to identify and investigate the biaxial mechanical behavior of elastic and muscular arteries (Saravanan, Baek, Rajagopal, & Humphrey, 2006). That is because through inflation test one could investigate physiologically meaningful mechanical conditions by preserving the native geometry of the vessel and mimicking the *in vivo* loading conditions during testing (Macrae, Miller, & Doyle, 2016). Comparably, biaxial extension test is better able to characterize the anisotropic behavior of an artery, since both circumferential and longitudinal directions are loaded simultaneously (Humphrey, 1995; Sacks & Sun, 2003). Also, the applied force and the amount of stretch in circumferential and longitudinal direction can be controlled, allowing the in vivo state simulation under physiological condition (Tian & Chester, 2012). Genetic modification and constituent purification combined with extension test is another approach that focus on analyzing the mechanics and microstructure of the isolated tissue. In 1998, Lillie and Gosline (Lillie, David, & Gosline, 1998) compared the behavior of purified elastin with and without its microfibrils by autoclaving procedures, in order to determine the contribution of the microfibrils to the performance of entire elastin meshwork.

In addition to pressure-diameter and stress-strain relationship obtained via *in vitro* measurements, hemodynamic factors could also be monitored through *in vivo* measurements. Many clinical studies expressed interests on determining the pulse wave velocity and pulse pressure associated aortic stiffening due to microstructural changes (Mitchell, 2009). However, the current pulse wave velocity estimation is only capable of representing an average global

relationship between two remote measurement location due to lacking of the exact arterial geometry (Vappou, Luo, & Konofagou, 2010).

CHAPTER 2: Mechanical characterization of damage behavior in the pulmonary artery

2.1 Introduction

We perform an *in vitro* cyclic inflation tests to characterize the elastic mechanical behavior of porcine pulmonary arteries, and the effect of irreversible damage. Specifically, we analyze the pressure-diameter relationship before and after an over-pressurization to understand the onset of the mechanical damage. Moreover, we use an elastic constitutive model of the arterial wall, which consists of two collagen fiber families and an isotropic elastin matrix (Bellini et al., 2014; Gerhard A. Holzapfel, Gasser, & Ogden, 2000), to quantitatively compare the mechanical properties control and damaged specimens. Finally, the pressure-induced changes in micro-structural configuration of the pulmonary arteries are studied using histological images

2.2 Methods

2.2.1 Specimen preparation

Chest cavities (i.e., heart, lungs, trachea, esophagus) are obtained from six adult, male pigs from the MEAT laboratory at Michigan State University, and then stored at -20°C for up to two weeks. Prior to testing, samples are defrosted at room temperature for 24 hours, then the PA is separated from the right ventricle and from the aorta by removing the connective tissue. We then isolated the PA from the lungs, up to the second bifurcation, which allowed us to identify a right and left branch. One of the branches was selected for mechanical testing, randomized between left and right, while a ring was cut from the other branch for histology. Before mechanical tests, small branches are sutured to allow pressurization of the sample, up to obtain a length of ~ 10cm for the overall sample. The samples were then stored in Hank's balanced salt solution (HBSS) in the fridge.

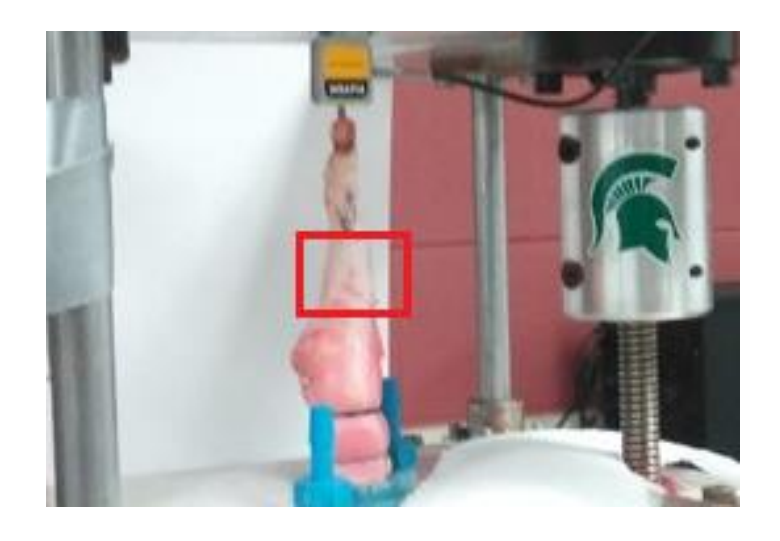


Figure 4. Inflation-extension testing device with specimen mounted in between

2.2.2 Mechanical testing

Before mounting the samples for pressurization, geometrical characteristics have been recorded. Specifically, we recorded each sample's thickness at 4 different locations, along the circumferential direction, and total axial length, employing a Vernier caliper. Mechanical tests were carried out in a custom-built inflation-extension testing device, as previously published (Kim & Baek, 2011). The system has the capability to apply, simultaneously, axial pre-stretch via a linear motor, and luminal pressure via a remote controlled syringe pump. The samples' diameter was then recorder throughout the test using a CCD camera (Hitachi KP-M2A), while the pressure was measured using a pressure transducer (Honeywell FP2000). The fluid used for pressurization was NaCl solution (9%).

The main branch of the PA specimen was secured to a cannula on one end, to allow pressurization, and to a vertically placed support on the other end. The axial pre-stretch was adjusted to ~ 10% of the original length. Using a custom LabVIEW program, we subjected each sample to the biaxial testing protocols consisting of three parts. After preconditioning, which consisted in 5 cycles of pressurization from 0 to 30 mmHg, each vessel was pressurized for three

sets of 10 loading – unloading cycles, as follows: first, from 0 to 50 mmHg (part 1); second, from 0 to 100 mmHg, to induce damage (part 2); and third, for 0 to 50 mmHg (part 3). **Figure 5** shows the pressure – diameter data over the course of the mechanical test for one representative specimen. The protocol also included a 1-minute recovery period between each two successive parts of the test. We used the pressure-diameter curves collected during part 1 of the test to identify mechanical behavior of the vessels before damage, and the curves collected during part 3 of the test to identify the mechanical behavior of the vessels after damage. After testing, we repeated the measure of thickness and axial length.

2.2.3 Histological analysis

Sections from samples collected before damage (from the untested PA branch) and after damage (from the PA tested branch, after completion of the test) were processed for histological analysis. Briefly, the samples were fixed in a 10% formalin solution for an hour and then stored at room temperature in 30% ethanol before being embedded in paraffin and sectioned. Sectioning and staining were carried out by the MSU Histopathology Lab. Histological analysis were focused on determining changes in the collagen fiber's and elastin's structure, by comparing samples collected before and after damage. To analyze collagen fibers' integrity, we stained the samples using picrosirius red (PSR) and we imaged them with polarized light. Finally, to investigate the elastin's structure we employed the Verhoeff-van Gieson (VVG) stain.

2.2.4 Mechanical model

The structural properties of the control and damaged PA specimens are characterized using a non-linear hyperelastic model to determine the constituent-wise indications of the damage. Assuming an incompressible material, the Cauchy stress can be computed as

$$\mathbf{T} = -p\mathbf{I} + 2\mathbf{F} \frac{\partial W}{\partial \mathbf{c}} \mathbf{F}^T \tag{12}$$

where p is the Lagrange multiplier enforcing incompressibility, and \mathbf{F} and \mathbf{C} are the deformation gradient and right Cauchy-Green tensor, respectively. In addition, W is the stored elastic strain energy in the material. Histological analyses on the arteries showed that the arterial wall is comprised of layers of elastin and collagen fibers. Mechanical response of the elastin content of the arterial wall is predominantly isotropic (Gundiah, Ratcliffe, & Pruitt, 2009), and thus is modeled as a neo-Hookean material. Alternatively, the contribution of collagen fibers to the anisotropic part of the mechanical response is modeled as an exponential function, proposed by (Gerhard A. Holzapfel et al., 2000).

The total strain energy function can be written as a summation of two contributions

$$W = \frac{c_1}{2}(I_1 - 2) + \sum_{K=1,2} \frac{c_1^k}{4c_2^k} \{ exp[c_2^k(\lambda^k)^2 - 1)^2] - 1 \}, \tag{13}$$

where the superscript k denotes the k-th fiber family; c_1, c_1^k , and c_2^k are material parameters (in this study $c_1^1 = c_1^2 = c_1^{1,2}$ and $c_2^1 = c_2^2 = c_2^{1,2}$); I_1 is the first invariant of the right Cauchy-Green tensor (i.e. Tr C). Finally, the stretch ratio of the k-th fiber family is defined as $\lambda^k = \sqrt{\lambda_\theta^2 sin^2 \alpha^k + \lambda_z^2 cos^2 \alpha^k}$, where α^k is the angle between each fiber family direction and the axial direction (here $\alpha = \alpha^1 = \alpha^2$).

In this study, we aim to quantify the mechanical changes associated with damage due to supraphysiological pressure. Therefore, we decided to use the same constitutive form to describe samples before and after damage. Best-fit values for the 4 model parameters $(C_1, c_1^{1,2}, c_2^{1,2}, \alpha)$ have been determined separately for each specimen in the before and after damage conditions specimen. Specifically, using a fminsearch function (MATLAB), we minimized the objective function (Baek, Gleason, Rajagopal, & Humphrey, 2007).

20

$$e = \sqrt{\frac{\sum (P_{est} - P_{data})^2}{\sum (P_{data})^2}} + \kappa (\lambda_z - \overline{\lambda_z})^2$$
 (14)

where P_{data} and P_{est} are the measured and computed intramural pressure, respectively. Moreover, the axial stretch in the experiments are fixed to be ~10% with respect to the unloaded control specimen ($\lambda_z = 1.1$). Therefore, this constraint is added to the objective function with a Lagrangian multiplier κ . It is worthy to note that for each specimen, the first loading curve from part 1 (control) and 3 (after damage) are used for parameter estimation.

2.3 Results

Of the six samples tested, only five were considered for our analysis; one sample was discarded due to excessive noise in the data. Pre-test measurements of samples showed initial length of 117.90 ± 13.8 mm, wall thickness of 0.89 ± 0.063 mm, and initial outer diameter of 13.71 ± 2.42 mm. Post-test measurements concluded that there was no significant change in the overall length of the specimens, whereas, the average wall thickness decreased to 0.79 ± 0.044 mm.

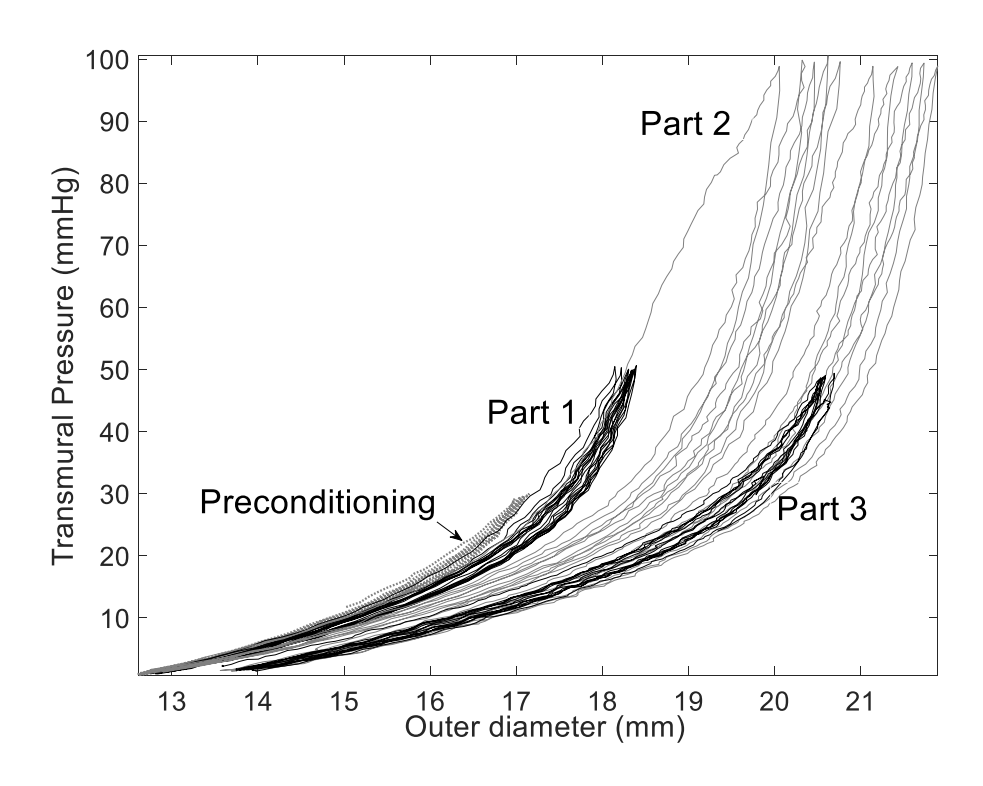


Figure 5. Luminal pressure and outer diameter raw data for a representative sample, as collected throughout the mechanical test. Specifically, part 1 (dark gray line) describes the mechanical behavior of the PA before the damage, part 2 (light gray line) describes the response to over-pressurization which generates damage within the wall, and part 3 (dark gray line) describes the mechanical behavior of the PA after damage. Also shown, the preconditioning protocol (dotted light gray line).

In **Figure 5** we show a representative set of raw pressure-diameter data as collected throughout the mechanical test. During the initial mechanical test (part 1), the vessel exhibited quasi-elastic characteristics, showing repeatable behavior for consecutive loading cycles. In the following, we will refer to the first loading curve of this portion of the test as the before-damage behavior of the PAs. During over-pressurization (part 2), conversely, we observed a pronounced rightward shift of each consecutive loading cycle, which suggests the development of mechanical damage within the arterial wall. Finally, in part 3 of the test, the vessel displayed some level of recovery of the elastic behavior, shown by the fact that consecutive loading cycles generate repeatable curves. All

specimens, however, showed qualitatively a significant increase in diameter for each value of pressure, when comparing curves from part 1 to curves from part 3 of the test. This seems to confirm the hypothesis that the application of supra-physiological pressures can damage the arterial wall in a potentially permanent way. In the following, we will refer to the first loading curve of part 3 of the test as the after-damage behavior of the PAs.

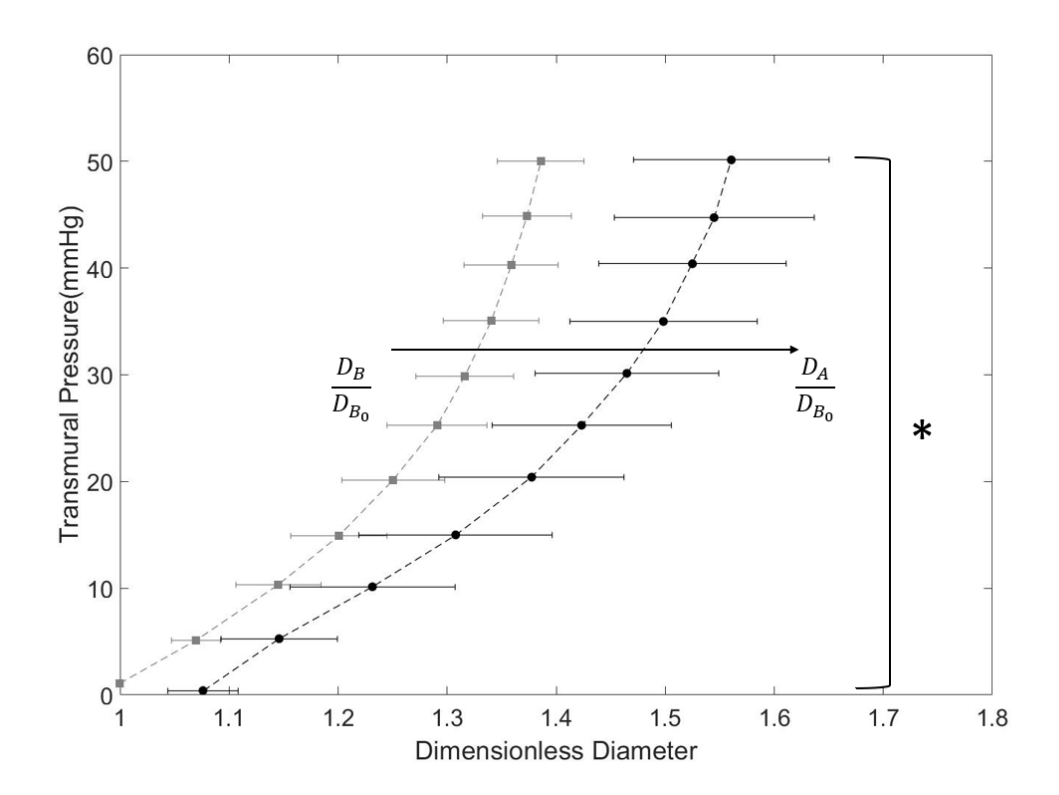


Figure 6. Average pressure vs. normalized diameter curve for all specimens. D_B and D_A correspond to before and after damage diameters, respectively. The before damage behaviors have been collected during the first loading of part 1 of the test, while the after damage behavior have been collected during part 3 of the test. The asterisk indicates that the normalized diameters were significantly different, at p < 0:05, when comparing before and after damage behaviors.

We then quantified the diameter increase associated with over-pressurization by comparing diameters before and after damage, for each value of pressure. First, we normalized the diameter values recorded throughout the test by the diameter value at zero pressure after preconditioning, for each sample. Then, we performed an across-sample average of the normalized diameter before damage (i.e., D_B/D_{B_0}) and after damage (i.e., D_A/D_{B_0}) for values of pressures included between 0 and 50 mmHg, shown in **Figure 6**. Statistical analysis confirms that the normalized diameter increase observed when comparing before and after damage behaviors is significant (p < 0.05 for

each value of pressure). The damaged specimens showed an enlargement amounting to ~20% of the diameter.

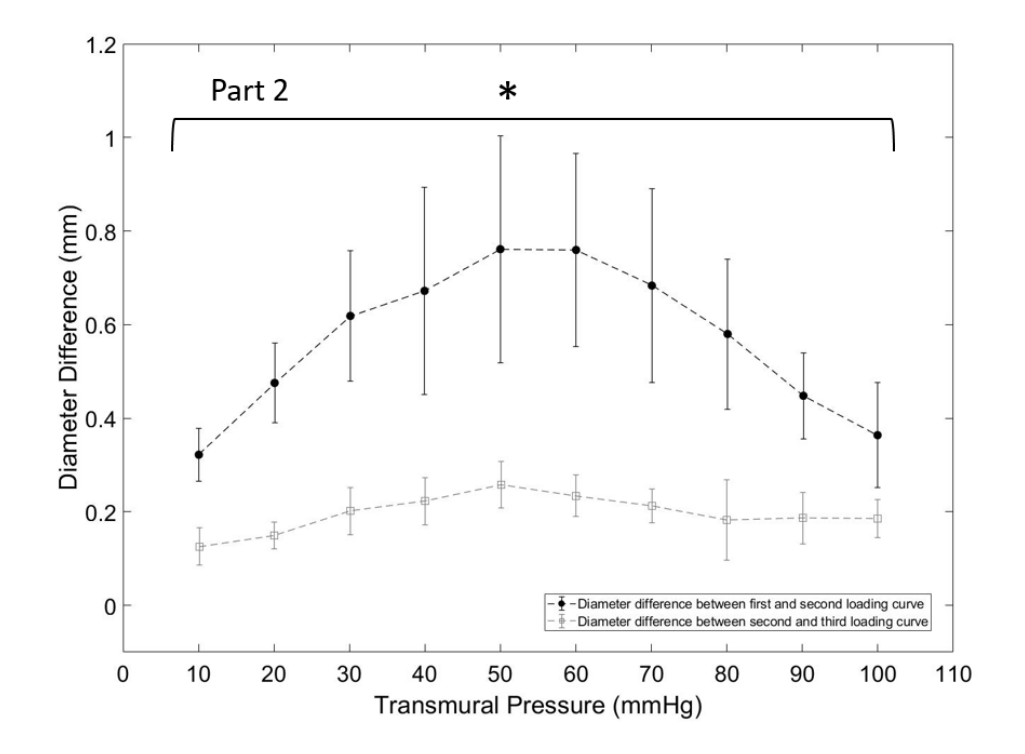


Figure 7. Change in diameter during different loading curves. Black circles represent that diameter difference between the first and second loading curve of part 2 of the test, gray squares represent the difference in diameter between the second and third loading curve. The * indicates that the diameters were significantly different at p < 0:05.

In an effort to identify the pressure for which the damage start occurring, we compared the first three consecutive loading curves for part 2 of the test. Specifically, the difference between diameters of the first and second loading curves, and the difference between diameters of the second and third loading curves are compared in **Figure 7**. A significant softening behavior can be observed during the first over-pressurization to 100 mmHg. Arteries are enlarged after the first loading cycle, while the change in size is significantly smaller over the next cycles. This result confirms that the irreversible damage of mechanical behavior was caused by a high pressure.

Particularly, a pressure of 50-60 mmHg, where the diameter difference is the largest, seems to be a reasonable candidate to quantify the onset of damage. However, it is not clear if mechanical damage were present during part 1 of the test.

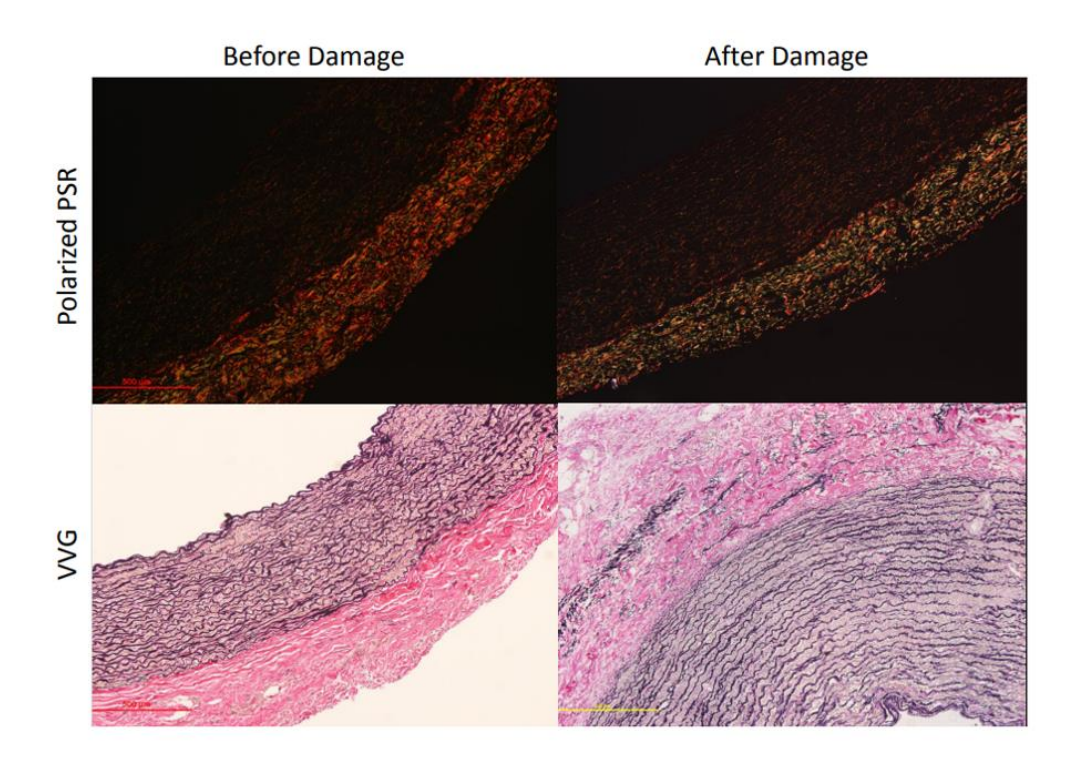


Figure 8. 4 Histology images of tissue samples from the PA. Top row: Picrosirius red under polarized light (collagen fibers in red, yellow and green); bottom row: VVG (elastin in black, nuclei in purple, and cytoplasm in pink). Left: before damage samples; right: after damage samples. Bar in each image represents 500 μm.

Figure 8 shows histological images of a representative specimens, before and after damage. Polarized PSR images show a color shift from bright red (larger diameters fibers) to yellow-green fibers (smaller diameter fibers), which could indicate damaged in collagen fibers. On the other hand, although the elastin sheets appear to be more dispersed in the VVG stained image of the damaged specimen, there are no clear qualitative indications of increased damage in the elastin fiber network.

Finally, the model describes the results accurately, according to the computed R^2 , for both the before and after damage specimens, as shown in **Table 1**. Collagen fiber stiffness parameter, c1,2 2, and the fiber directions α seem to incur the most changes during the over-pressurization of arteries which is consistent with the observation in histology images. The results indicate a softening in collagen fibers with approximately 62% decrease in the dimensionless material parameter. Conversely, the fiber orientation seems to have altered towards the axial direction. It is worthy to note that the stiffness of elastin has decreased by 41% on average, although a statistically significant difference was not observed.

Table 1. Best-fit material parameters for the 2-fiber family model and estimated axial stretch.

	Specimen\Parameters	$c_1(kPa)$	$c_1^{1,2}({\rm kPa})$	$c_2^{1,2}$	$\alpha(\deg)$	R^2
Control	1	18.04	5.36	8.97	53.66	0.97
	2	17.38	7.65	5.55	52.07	0.99
	3	13.42	26.75	4.73	53.69	0.98
	4	10.99	19.01	3.25	52.80	0.99
	5	16.63	14.48	2.996	50.94	0.98
	$avg. \pm std$	15.29 ± 2.99	14.65 ± 8.67	5.10 ± 2.41	$52.63{\pm}1.16$	
Damaged	1	5.51	13.49	1.70	45.34	0.99
	2	8.01	12.43	2.07	45.78	0.98
	3	12.32	28.50	2.70	50.71	0.98
	4	2.75	24.86	1.10	46.73	0.99
	5	16.09	14.08	2.11	46.92	0.99
	$avg. \pm std$	$8.94{\pm}5.33$	18.67 ± 7.45	1.94 ± 0.69	47.10 ± 2.12	
	% change	-41.56	27.45	-62.03*	-10.52*	

The superscript * indicates significant difference at p < 0.05.

2.4 Discussion

Characterizing dissipative behavior of vasculature, such as softening and damage, is an emerging area of research, in predicting potential risk of diseases and elucidating mechanisms of disease progression. Previous studies have investigated the mechanical behavior of arteries in pressures

higher than physiological range (e.g., over 150 mmHg) mostly in the systemic circulation systems whereas lumen enlargement is not a common feature of the hypertensive patients. On the other hand, a larger caliber of the vessels in the lungs is a characteristic feature of PH patients when compared to healthy individuals, e.g., 20% larger arterial diameter in adult PH patients and 30% larger arterial diameter in pediatric PH patients. The central hypothesis that we sought to test in this study is that over-pressurization could lead to a permanent increase in the luminal diameter of proximal pulmonary arteries. To this end, we designed a mechanical testing protocol to characterizing the change in mechanical behaviors of porcine PA in response to damage. Then, we employed a microstructurally inspired constitutive law to interpret the results and make hypothesize which tissue components could be more affected by the damage process. Finally, we employed histological images to qualitatively support the proposed damage mechanisms.

While previous studies have investigated the irreversible mechanical response of the arteries both in physiological and pathological conditions (Scott, Ferguson, & Roach, 1972), to the authors' knowledge, this study is first to investigate the mechanical damage in the pulmonary arteries. Large pulmonary arteries are main conduits in a low-pressure system, in comparison to the systemic circulation, and this physiological function could result in a significantly different structure when compared to other elastic vessels. For example, in cerebral arterial tissues, the mechanical response to cyclic loading to a maximum pressure of 100 mmHg was shown to have no effect on the pressure diameter curves (D. Li & Robertson, 2009. In this study we showed that in PAs, however, a pressure of 100 mmHg appeared to induce an irreversible effect on the mechanical behavior of the wall (**Figure 5**). Furthermore, the mechanical test we performed showed that preconditioning to a pressure of 30 mmHg did not change the mechanical behavior of the artery significantly, indicating that no damage incurred for this pressure level. In addition, a

relatively small softening behavior is observed in part 1 of the tests, where the highest pressure is 50 mmHg (data not shown, not significant). However, our results indicated that a more pronounced damage across all 5 specimens was associated with part 2 of the test (**Figure 6**), where all of the vessels have a significantly larger caliber after the inflation test (p<0.05). The results of part 3 demonstrated that after the over-pressurization, the arterial wall is more compliant, yet the cyclic pressure-diameter curves exhibit an elastic behavior. Schriefl et al (Schriefl et al., 2015), observed similar softer but elastic behavior when the arterial collagen was enzymatically removed in human abdominal aorta samples.

The compliant behavior is also reflected in terms of the material parameters in Table 1, where the parameter $c_2^{1,2}$ significantly decreases, when compare before and after damage samples. The parameters $c_1^{1,2}$ and $c_2^{1,2}$ represent, in the model employed here, the constitutive properties of the collagen in the arterial wall as well as its effectiveness at different pressure domains (Roach & Burton, 1957). The significantly large difference between the first-second and second-third consecutive loading curves during part 2 of the test demonstrate that a pressure higher than 50 mmHg induces sudden irreversible changes in the structure of the pulmonary arteries, whereas the pressure below 50 mmHg induced relatively smaller mechanical damage (**Figure 7**). Specifically, the abrupt change in the slope of the curve suggest that the damaging pressure is ~ 60 mmHg. The continuous softening behavior throughout part 2 may imply that the damage threshold in each following sets of loading curves may be decreasing. However, this behavior may be due to a constant softening in the arterial structure. Table 1 suggests also that the collagen fiber directions could significantly change before and after damage. Particularly, the angle α , the angle between the effective fiber orientation with respect to the axial direction of the artery, show an average 5° decrease in the fiber orientation, which could suggest that the circumferentially oriented collagen fibers are damaged. Similarly, Converse et al. (Converse et al., 2018) observed that the direction of the damage conforms to the direction of the over-stretch using a collagen hybridizing peptide in the ovine middle cerebral artery specimens. Furthermore, our histology images also suggested that the collagen fibers are could be significantly damaged by over-pressurization, reinforcing our modeling prediction.

This study has some limitations. First, the tests were performed in open air and room temperature, while other studies perform the tensile tests in a saline solution (Schrauwen et al., 2012). Second, we did not account for mechanical response (active or passive) of smooth muscle cells in our study. Third, while we kept the specimens axially stretched at 10%, we did not measure the axial force induced in the specimens during the pressurization. Fourth, we assumed that the damaged specimens have are fully elastic, i.e., we did not use a damage model in our constitutive relations. Despite these limitations, this is the first study to investigate the mechanical damage as a result of over-pressurization in the pulmonary arteries.

2.5 Conclusion

PH is a complex and multifaceted disease in which the structure of the proximal PAs changes as a result of a variety of biomechanical and biochemical factors. In this study, we aimed to analyze only the mechanical response of the proximal PAs under elevated pressure. The results presented here suggest that mechanical damage of the arterial wall, associated with significantly increased blood pressure, could be contributing to the pathology of PH. Furthermore, the combination of model and histological images, seem to suggest that the damage is localized in the collagen fibers network in the adventitial layer

BIBLIOGRAPHY

BIBLIOGRAPHY

- 1. Akhtar, R., Sherratt, M. J., Cruickshank, J. K., & Derby, B. (2011). Characterizing the elastic properties of tissues. *Materials Today*, *14*(3), 96–105. https://doi.org/10.1016/S1369-7021(11)70059-1
- 2. Armentano, R. L., Levenson, J., Barra, J. G., Fisher, E. I., Breitbart, G. J., Pichel, R. H., & Simon, A. (1991). Assessment of elastin and collagen contribution to aortic elasticity in conscious dogs. *The American Journal of Physiology*, 260, H1870-7.
- 3. Botney, M. D. (1999). Role of Hemodynamics in Pulmonary Vascular Remodeling. *American Journal of Respiratory and Critical Care Medicine*, *159*(2), 361–364. https://doi.org/10.1164/ajrccm.159.2.9805075
- 4. Chuong, C. J., & Fung, Y. C. (1983). Three-Dimensional Stress Distribution in Arteries. *Journal of Biomechanical Engineering*, 105(3), 268–274. https://doi.org/10.1115/1.3138417
- 5. Delfino, A., Stergiopulos, N., Moore, J. E., & Meister, J.-J. (1997). Residual strain effects on the stress field in a thick wall finite element model of the human carotid bifurcation. *Journal of Biomechanics*, 30(8), 777–786. https://doi.org/10.1016/S0021-9290(97)00025-0
- 6. Edwards, P. D., Bull, R. K., & Coulden, R. (1998). CT measurement of main pulmonary artery diameter. *The British Journal of Radiology*, 71(850), 1018–1020. https://doi.org/10.1259/bjr.71.850.10211060
- 7. Faury, G., Pezet, M., Knutsen, R. H., Boyle, W. A., Heximer, S. P., McLean, S. E., ... Mecham, R. P. (2003). Developmental adaptation of the mouse cardiovascular system to elastin haploinsufficiency. *The Journal of Clinical Investigation*, *112*(9), 1419–1428. https://doi.org/10.1172/JCI19028
- 8. Ferrara, A., & Pandolfi, A. (2008). Numerical modelling of fracture in human arteries. *Computer Methods in Biomechanics and Biomedical Engineering*, 11, 553–567.
- 9. Holzapfel, G. A., Gasser, T. G., & Ogden, R. W. (2000). A new constitutive framework for arterial wall mechanics and a comparative study of material models. *Journal of Elasticity*, 61, 1–48.
- 10. Humphrey, J. D. (1995). Mechanics of the arterial wall: review and directions. *Critical Reviews in Biomedical Engineering*, 23(1–2), 1–162.
- 11. Humphrey, J. D., Baek, S., & Niklason, L. E. (2007). Biochemomechanics of cerebral vasospasm and its resolution: I. A new hypothesis and theoretical framework. *Annals of Biomedical Engineering*, *35*, 1485–1497.
- 12. Humphrey, J. D., & Tellides, G. (2018). Central artery stiffness and thoracic aortopathy. *American Journal of Physiology-Heart and Circulatory Physiology*, *316*(1), H169–H182. https://doi.org/10.1152/ajpheart.00205.2018

- 13. Hunter, K. S., Lammers, S. R., & Shandas, R. (2011). Pulmonary Vascular Stiffness: Measurement, Modeling, and Implications in Normal and Hypertensive Pulmonary Circulations. *Comprehensive Physiology*, *1*(3), 1413–1435. https://doi.org/10.1002/cphy.c100005
- 14. Kim, J., & Baek, S. (2011). Circumferential variations of mechanical behavior of the porcine thoracic aorta during the inflation test. *Journal of Biomechanics*, 44(10).
- 15. Lammers, S., Scott, D., Hunter, K., Tan, W., Shandas, R., & Stenmark, K. R. (2012). Mechanics and Function of the Pulmonary Vasculature: Implications for Pulmonary Vascular Disease and Right Ventricular Function. In *Comprehensive Physiology* (pp. 295–319). https://doi.org/10.1002/cphy.c100070
- 16. Li Zhihe, Froehlich Jeffrey, Galis Zorina S., & Lakatta Edward G. (1999). Increased Expression of Matrix Metalloproteinase-2 in the Thickened Intima of Aged Rats. *Hypertension*, *33*(1), 116–123. https://doi.org/10.1161/01.HYP.33.1.116
- 17. Macrae, R. A., Miller, K., & Doyle, B. J. (2016). Methods in Mechanical Testing of Arterial Tissue: A Review. *Strain*, *52*(5), 380–399. https://doi.org/10.1111/str.12183
- 18. Mehari, A., Valle, O., & Gillum, R. F. (2014). Trends in Pulmonary Hypertension Mortality and Morbidity. *Pulmonary Medicine*, 2014. https://doi.org/10.1155/2014/105864
- 19. Nickel, N. P., Spiekerkoetter, E., Gu, M., Li, C. G., Li, H., Kaschwich, M., ... Rabinovitch, M. (2015). Elafin Reverses Pulmonary Hypertension via Caveolin-1-Dependent Bone Morphogenetic Protein Signaling. *American Journal of Respiratory and Critical Care Medicine*, 191(11), 1273–1286. https://doi.org/10.1164/rccm.201412-2291OC
- 20. Roach, M. R., & Burton, A. C. (1957). THE REASON FOR THE SHAPE OF THE DISTENSIBILITY CURVES OF ARTERIES. *Canadian Journal of Biochemistry and Physiology*, *35*(8), 681–690. https://doi.org/10.1139/o57-080
- 21. Rounds, S., & Hill, N. S. (1984). Pulmonary Hypertensive Diseases. *Chest*, 85(3), 397–405. https://doi.org/10.1378/chest.85.3.397
- 22. Sanz, J., Kariisa, M., Dellegrottaglie, S., Prat-González, S., Garcia, M. J., Fuster, V., & Rajagopalan, S. (2009). Evaluation of Pulmonary Artery Stiffness in Pulmonary Hypertension With Cardiac Magnetic Resonance. *JACC: Cardiovascular Imaging*, 2(3), 286–295. https://doi.org/10.1016/j.jcmg.2008.08.007
- 23. Saravanan, U., Baek, S., Rajagopal, K. R., & Humphrey, J. D. (2006). On the Deformation of the Circumflex Coronary Artery During Inflation Tests at Constant Length. *Experimental Mechanics*, 46(5), 647–656. https://doi.org/10.1007/s11340-006-9036-2
- 24. Schrauwen, J. T. C., Vilanova, A., Rezakhaniha, R., Stergiopulos, N., van de Vosse, F. N., & Bovendeerd, P. H. M. (2012). A method for the quantification of the pressure dependent 3D collagen configuration in the arterial adventitia. *Journal of Structural Biology*, *180*(2), 335–342. https://doi.org/10.1016/J.JSB.2012.06.007

- 25. Schriefl, A. J., Schmidt, T., Balzani, D., Sommer, G., & Holzapfel, G. A. (2015). Selective enzymatic removal of elastin and collagen from human abdominal aortas: Uniaxial mechanical response and constitutive modeling. *Acta Biomaterialia*, *17*, 125–136. https://doi.org/10.1016/J.ACTBIO.2015.01.003
- 26. Sheidaei, A., Hunley, S. C., Raguin, L. G., & Baek, S. (2009). Simulation of abdominal aortic aneurysm growth with updating hemodynamic loads using a realistic geometry. *ASME J. Biomech. Eng.*
- 27. Sho, E., Sho, M., Hoshima, K., Kimura, H., Nakahashi, T. K., & Dalman, R. L. (2004). Hemodynamic forces regulate mural macrophage infiltration in experimental aortic aneurysms. *Experimental and Molecular Pathology*, 76, 108–116.
- 28. Stepnowska, E., Lewicka, E., Dąbrowska-Kugacka, A., Miękus, P., & Raczak, G. (2017). Prognostic factors in pulmonary arterial hypertension: Literature review. *Advances in Clinical and Experimental Medicine*, 26(3), 549–553. https://doi.org/10.17219/acem/61855
- 29. Takamizawa, K., & Hayashi, K. (1987). Strain energy density function and uniform strain hypothesis for arterial mechanics. *Journal of Biomechanics*, 20(1), 7–17. https://doi.org/10.1016/0021-9290(87)90262-4
- 30. Thubrikar, M. J., & Robicsek, F. (1995). Pressure-induced arterial wall stress and atherosclerosis. *The Annals of Thoracic Surgery*, *59*(6), 1594–1603. https://doi.org/10.1016/0003-4975(94)01037-D
- 31. Truong, U., Fonseca, B., Dunning, J., Burgett, S., Lanning, C., Ivy, D. D., ... Barker, A. J. (2013). Wall shear stress measured by phase contrast cardiovascular magnetic resonance in children and adolescents with pulmonary arterial hypertension. *Journal of Cardiovascular Magnetic Resonance*, 15(1), 81. https://doi.org/10.1186/1532-429X-15-81
- 32. Tuder, R. M., Marecki, J. C., Richter, A., Fijalkowska, I., & Flores, S. (2007). Pathology of Pulmonary Hypertension. *Clinics in Chest Medicine*, 28(1), 23–vii. https://doi.org/10.1016/j.ccm.2006.11.010
- 33. Valentín A, Cardamone L, Baek S, & Humphrey J.D. (2009). Complementary vasoactivity and matrix remodelling in arterial adaptations to altered flow and pressure. *Journal of The Royal Society Interface*, 6(32), 293–306. https://doi.org/10.1098/rsif.2008.0254
- 34. Vorp, D. A., Wang, D. H. J., Webster, M. W., & Federspiel, W. J. (1998). Effect of intraluminal thrombus thickness and bulge diameter on the oxygen diffusion in abdominal aortic aneurysm. *Journal of Biomechanical Engineering*, *120*, 579–583.
- 35. Wagenseil, J. E., & Mecham, R. P. (2012). Elastin in large artery stiffness and hypertension. *Journal of Cardiovascular Translational Research*, *5*, 264–273.

- 36. Wagenseil, Jessica E., Ciliberto, C. H., Knutsen, R. H., Levy, M. A., Kovacs, A., & Mecham, R. P. (2010). The importance of elastin to aortic development in mice. *American Journal of Physiology-Heart and Circulatory Physiology*, 299(2), H257–H264. https://doi.org/10.1152/ajpheart.00194.2010
- 37. Wagenseil Jessica E., Ciliberto Chris H., Knutsen Russell H., Levy Marilyn A., Kovacs Attila, & Mecham Robert P. (2009). Reduced Vessel Elasticity Alters Cardiovascular Structure and Function in Newborn Mice. *Circulation Research*, *104*(10), 1217–1224. https://doi.org/10.1161/CIRCRESAHA.108.192054
- 38. Wagenseil, Jessica E., Nerurkar, N. L., Knutsen, R. H., Okamoto, R. J., Li, D. Y., & Mecham, R. P. (2005). Effects of elastin haploinsufficiency on the mechanical behavior of mouse arteries. *American Journal of Physiology-Heart and Circulatory Physiology*, 289(3), H1209–H1217. https://doi.org/10.1152/ajpheart.00046.2005
- 39. Wulandana, R., & Robertson, A. M. (2005). An inelastic multi-mechanism constitutive equation for cerebral arterial tissue. *Biomech. Model Mechanobiol.*, *4*, 235–248.
- 40. Zambrano, B. A., Gharahi, H., Lim, C. Y., Jaberi, F. A., Choi, J., Lee, W., & Baek, S. (2016). Association of Intraluminal Thrombus, Hemodynamic Forces, and Abdominal Aortic Aneurysm Expansion Using Longitudinal CT Images. *Annals of Biomedical Engineering*,